Developed Turbulent Transport in Ducts for Large Prandtl or Schmidt Numbers

OWEN T. HANNA and ORVILLE C. SANDALL

Department of Chemical and Nuclear Engineering
University of California, Santa Barbara, California 93106

The problem of developed turbulent heat or mass transfer in a duct is considered for the limit of large σ (Prandtl or Schmidt number). The limiting results depend on the behavior of the eddy diffusivity near the solid surface. Since there is a question about whether this variation begins with $\epsilon \propto y^{+3} + \ldots$ or $\epsilon \propto y^{+4} + \ldots$ for y^+ near zero, both possibilities are considered. In each case the first three terms of the asymptotic expansion for $\sigma \to \infty$ are obtained. The first term of the asymptotic expansion agrees with limiting results derived earlier, while the correction terms indicate the errors associated with earlier simplifying assumptions.

By proper scaling, it is demonstrated that in the limit of $\sigma \to \infty$ the results are independent of geometry and boundary conditions for situations involving parallel plates, circular tubes and concentric annuli with either constant surface heat flux or temperature. The correction terms to the $\sigma \to \infty$ asymptote can be significant, although the effect of Reynolds number on the correction terms is very small.

A comparison between a typical numerical integration and the asymptotic formula shows excellent agreement. The asymptotic formulae are used to correlate large Schmidt number mass transfer data.

Heat or mass transfer under developed conditions for turbulent flow in ducts has long been of practical interest. This is true since for many transport situations in turbulent flow the temperature or concentration achieves its developed profile over most of the transfer region. The particular case where $\sigma \to \infty$ has been of special interest both theoretically and in practice, since for heat or mass transfer in many liquids the σ values are large.

Early work on this problem was based on the analogies of Prandtl-Taylor, von Kármán, and Martinelli (*8*). The differences between these analogies are attributable to various simplifying assumptions made by the authors. Subsequently, Lyon (*10*) and Seban and Shimazaki (*11*) presented analyses which were devoid of simplifying assumptions, but which could only be implemented numerically. The main purpose of this paper is the development of an asymptotic expansion for the rigorous formulation in the limit of $\sigma \to \infty$.

Deissler (*2*) used the idea of a continuously varying eddy diffusivity to determine an analytical approximation for the Stanton number in a circular tube for the limit of $\sigma \to \infty$. Later Elrod (*3*) showed that the Taylor series expansion for the eddy diffusivity in the neighborhood of the wall must begin with a term proportional to y^n where n must be greater than or equal to three. The asymptotic dependence of the Stanton number on σ for $\sigma \to \infty$ depends on this value of n. Empirical correlations based on values of n of three (*4, 9*) and four (*2, 12*) have been proposed, mainly of the form $St = A\, Re^a\, \sigma^b$. In addition, a number of large Schmidt number mass transfer experiments have been conducted with the goal of determining n. These investigations are not conclusive, since evidence is found for both $n = 3$ (*6, 7*) and $n = 4$ (*12*). Part of the reason for this discrepancy may be due to an inadequate formula with which to compare the experimental results.

In this paper we derive an asymptotic expansion of the Lyon equation for the limit of $\sigma \to \infty$. The expansion depends in a fundamental way on the eddy diffusivity variation near the wall. Since this variation is currently in question, both of the likely possibilities are considered. Three terms of the asymptotic expansion are generated for both $\epsilon(y^+) = K_3 y^{+3} + K_4 y^{+4} + K_5 y^{+5}$ and $\epsilon(y^+) = M_4 y^{+4} + M_5 y^{+5} + M_6 y^{+6}$. The errors due to taking only three terms of $\epsilon(y^+)$ are also estimated. The results show the corrections to earlier one-term approximations, and thereby indicate the validity of the corresponding simplifying assumptions as well as offering the means of achieving increased accuracy. The effects of geometry, boundary conditions, Schmidt number, and Reynolds number are considered for the cases of parallel plates, circular tubes, and concentric annuli under conditions of constant surface temperature or heat flux.

The formulae obtained should permit an accurate prediction of the Stanton number for $\sigma \to \infty$ and, in addition, should allow a discriminating interpretation of large Prandtl or Schmidt number experiments. Comparisons of the asymptotic results with both numerical calculations and mass transfer data are made later in the paper. The asymptotic expansions of the integrals describing the Stanton number are based on procedures given by Hanna (*5*).

DERIVATION OF EQUATIONS

Figure 1 illustrates the geometries and their respective coordinate systems for the three cases considered in this work. For the parallel plate geometry two different boundary conditions are considered: 1. constant but different wall temperatures, and 2. constant wall heat flux. For the circular tube and concentric annulus cases, the boundary condition considered is that of constant wall heat flux. The constant wall temperature boundary condition is considered in Appendix A,* where it is shown that for large σ the differences between the results for the constant flux and constant temperature boundary conditions become extremely small.

---

* Appendices have been deposited as Document No. 01763 with the National Auxiliary Publications Service (NAPS), c/o CCM Information Corp., 866 Third Ave., New York 10022 and may be obtained for $2.00 for microfiche or $5.00 for photocopies.

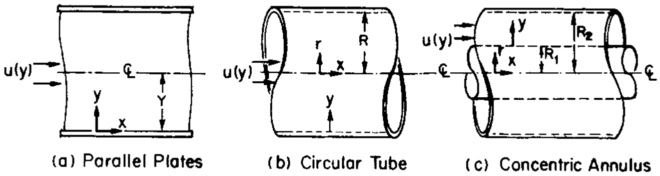

Fig. 1. Geometries considered for fully developed transport in ducts.

Parallel Plates

Constant but Different Wall Temperatures. For the parallel plate geometry the energy or mass conservation equation for constant physical properties and fully developed flow is

$$u^+ \frac{\partial \theta^+}{\partial x^+} = \frac{\partial}{\partial y^+} \left\{ \left(\frac{1}{\sigma} + \epsilon \right) \frac{\partial \theta^+}{\partial y^+} \right\} \quad (1)$$

where u^+ and y^+ are the usual universal velocity profile variables, and θ^+ refers to either the normalized temperature or concentration. Equation (1) neglects axial transport and includes the additional assumption of no viscous dissipation of energy in the case of heat transfer, or no diffusion induced normal velocity in the case of mass transfer. Also, we note that if the eddy diffusivities for energy transfer or mass diffusion are not equal to the eddy diffusivity for momentum, but if the ratio of these quantities is constant, then by means of proper scaling all of the succeeding results are applicable.

Sufficiently far downstream for the case considered here of constant and different wall temperatures, the temperature profile becomes fully developed and therefore $\partial \theta^+ / \partial x^+ = 0$. The boundary conditions may be expressed as

$$\begin{aligned} &\text{(i)} \quad y^+ = 0, \quad \theta^+ = 0 \\ &\text{(ii)} \quad y^+ = 2Y^+, \quad \theta^+ = 1.0 \end{aligned} \quad (2)$$

where

$$\theta^+ = \frac{\theta - \theta_1}{\theta_2 - \theta_1} \quad (3)$$

With these boundary conditions, Equation (1) may be integrated twice to yield

$$\theta^+ = \left\{ \int_0^{y^+} \frac{dz^+}{\frac{1}{\sigma} + \epsilon(z^+)} \right\} \Bigg/ \left\{ \int_0^{2Y^+} \frac{dz^+}{\frac{1}{\sigma} + \epsilon(z^+)} \right\} \quad (4)$$

The heat transfer coefficient is defined as

$$h = \frac{q_w}{\theta_b - \theta_1} \quad (5)$$

It may be shown that the bulk temperature for this case is just the arithmetic average of the wall temperatures, and thus the Stanton number may be expressed as

$$\frac{\sqrt{f/2}}{St} = \int_0^{Y^+} \frac{dz^+}{\frac{1}{\sigma} + \epsilon(z^+)} \quad (6)$$

Constant Wall Heat Flux. The case considered is for one wall insulated and the other wall with a constant heat flux. The boundary conditions for this situation may be written as

$$\begin{aligned} &\text{(i)} \quad x^+ = 0, \quad \theta^+ = 0 \\ &\text{(ii)} \quad y^+ = 0, \quad \frac{\partial \theta^+}{\partial y^+} = -1 \\ &\text{(iii)} \quad y^+ = 2Y^+, \quad \frac{\partial \theta^+}{\partial y^+} = 0 \end{aligned} \quad (7)$$

where

$$\theta^+ = \frac{k u^*}{q_w \nu} (\theta - \theta_0) \quad (8)$$

The result for constant but different fluxes on each wall may be obtained by superposition of two solutions of the type considered here.

Sufficiently far downstream θ^+ may be expressed as

$$\theta^+ = \alpha x^+ + \varphi(y^+) \quad (9)$$

The constant α may be determined from an overall energy balance to yield

$$\alpha = \frac{1}{\sigma Re} \quad (10)$$

With the temperature distribution given by Equation (9), Equation (1) may be integrated twice to give

$$\theta^+(x^+, y^+) - \theta^+(x^+, 0) = \frac{1}{\sigma Re} \int_0^{y^+} \frac{1}{\frac{1}{\sigma} + \epsilon(z^+)} \int_{2Y^+}^{z^+} u^+(w^+)\, dw^+\, dz^+ \quad (11)$$

The Stanton number becomes

$$\frac{\sqrt{f/2}}{St} = \frac{\sigma}{Re} \int_0^{2Y^+} u^+ \{\theta^+(x^+, y^+) - \theta^+(x^+, 0)\}\, dy^+ \quad (12)$$

Substitution of Equation (11) into Equation (12) and changing the order of integration gives the Lyon integral (*10*).

$$\frac{\sqrt{f/2}}{St} = \frac{1}{Re^2} \int_0^{2Y^+} \frac{1}{\frac{1}{\sigma} + \epsilon(y^+)} \left\{ \int_{y^+}^{2Y^+} u^+(z^+) dz^+ \right\}^2 dy^+ \quad (13)$$

Circular Tube, Constant Wall Heat Flux

For the circular tube geometry, the conservation equation in dimensionless form for the conditions of Equation (1) becomes

$$u^+ \frac{\partial \theta^+}{\partial x^+} = \frac{1}{r^+} \frac{\partial}{\partial r^+} \left\{ r^+ \left(\frac{1}{\sigma} + \epsilon \right) \frac{\partial \theta^+}{\partial r^+} \right\} \quad (14)$$

The constant wall heat flux boundary conditions are expressed as

$$\begin{aligned} &\text{(i)} \quad x^+ = 0, \quad \theta^+ = 0 \\ &\text{(ii)} \quad r^+ = 0, \quad \frac{\partial \theta^+}{\partial r^+} = 0 \\ &\text{(iii)} \quad r^+ = R^+, \quad \frac{\partial \theta^+}{\partial r^+} = 1 \end{aligned} \quad (15)$$

where

$$\theta^+ = \frac{k u^*}{q_w \nu} (\theta - \theta_0) \quad (16)$$

The Lyon integral expressing the fully developed Stanton number may be derived in an analogous manner as for Equation (13) for the parallel plate geometry to yield

$$\frac{\sqrt{f/2}}{St} = \frac{4}{Re^2} \int_0^{R^+}$$

$$\frac{\left\{ \int_{y^+}^{R^+} 2u^+ (z^+) \left(1 - \frac{z^+}{R^+}\right) dz^+ \right\}^2}{\left(1 - \frac{y^+}{R^+}\right) \left(\frac{1}{\sigma} + \epsilon(y^+)\right)} dy^+ \quad (17)$$

Concentric Annulus, Constant Wall Heat Flux

Two cases are considered for the concentric annulus geometry: 1. a constant flux on the inner wall with the outer wall insulated, and 2. a constant flux on the outer wall with the inner wall insulated. The result for any combination of constant wall heat fluxes may be obtained by superposing the two solutions considered here.

Constant Flux on Inner Wall, Outer Wall Insulated. The boundary conditions for this case may be written as

$$\begin{aligned} &\text{(i)} \quad x^+ = 0, \quad \theta^+ = 0 \\ &\text{(ii)} \quad r^+ = R_1^+, \quad \frac{\partial \theta^+}{\partial r^+} = -1 \\ &\text{(iii)} \quad r^+ = R_2^+, \quad \frac{\partial \theta^+}{\partial r^+} = 0 \end{aligned} \quad (18)$$

where

$$\theta^+ = \frac{k u_1^*}{q_w \nu} (\theta - \theta_0) \quad (19)$$

With these boundary conditions Equation (14) may be integrated for fully developed temperature profiles to yield

$$\frac{\sqrt{f_1/2}}{St} = \int_0^{R_2^+ - R_1^+} \frac{\left(\frac{4}{Re}\right)^2 \frac{R_1^+}{(R_1^+ + R_2^+)^2} \left\{ \int_{y^+}^{R_2^+ - R_1^+} u^+(z^+)(z^+ + R_1^+) dz^+ \right\}^2}{(y^+ + R_1^+) \left(\frac{1}{\sigma} + \epsilon(y^+)\right)} dy^+ \quad (20)$$

Constant Flux on Outer Wall, Inner Wall Insulated. The boundary conditions for this case may be written as

$$\begin{aligned} &\text{(i)} \quad x^+ = 0, \quad \theta^+ = 0 \\ &\text{(ii)} \quad r^+ = R_1^+, \quad \frac{\partial \theta^+}{\partial r^+} = 0 \\ &\text{(iii)} \quad r^+ = R_2^+, \quad \frac{\partial \theta^+}{\partial r^+} = -1 \end{aligned} \quad (21)$$

where

$$\theta^+ = \frac{k u_2^*}{q_w \nu} (\theta - \theta_0) \quad (22)$$

The Lyon integral for these conditions becomes

$$\frac{\sqrt{f_2/2}}{St} = \int_0^{R_2^+ - R_1^+} \frac{\left(\frac{4}{Re}\right)^2 \frac{R_2^+}{(R_1^+ + R_2^+)^2} \left\{ \int_{y^+}^{R_2^+ - R_1^+} u^+(z^+)(R_2^+ - z^+) dz^+ \right\}^2}{(R_2^+ - y^+) \left(\frac{1}{\sigma} + \epsilon(y^+)\right)} dy^+ \quad (23)$$

Method of Analysis

All of the turbulent heat transfer situations considered in this paper require the evaluation of I for some $G(y^+)$. The $G(y^+)$ functions depend on the particular situation being considered. The cases studied here are listed in Table 1. It is desired to determine several terms of the asymptotic representation of I for $\sigma \to \infty$, where $\epsilon(y^+)$ begins as $K_3 y^{+3} + K_4 y^{+4} \ldots$ or $M_4 y^{+4} + M_5 y^{+5} \ldots$.

Since we are interested in the behavior of I as $\sigma \to \infty$, the integrand of integral I must be examined in order to determine the region of maximum contribution. In all cases $G(y^+)$ is bounded in the region of integration, and since $\epsilon(y^+) \to 0$ for $y^+ \to 0$, we see that the maximum contribution to I for $\sigma \to \infty$ comes from near $y^+ = 0$. Thus it is natural to set up an approximation scheme which is valid near $y^+ = 0$. Also, it is apparent that for $\sigma \to \infty$, $I \to \infty$. The upper limit in the integrals defining the Stanton number is proportional to $Re \sqrt{f/2}$ according to Equations (13), (17), (20), and (22). In the expression for I, however, we have used an upper limit designated as L. The reason for this is that for the purpose of obtaining the $\sigma \to \infty$ asymptote, it is necessary to split the integral into two parts. This is required, since the power series approximations for $\epsilon(y^+)$ are not valid over the whole range of integration. It happens, as will be shown, that since the maximum contribution to the integral for $\sigma \to \infty$ comes from near $y^+ = 0$, the other part of the integral is relatively unimportant. Thus, the three-term asymptotic representations of I for $\sigma \to \infty$ given here are independent of the upper limit.

The procedure followed here is based on the successive extraction of the major contributions to the integral as a function of σ. The method was employed on an integral similar to I for turbulent boundary layer heat transfer (*5*).

$$\text{Asymptotic Evaluation of } \int_{y^+=0}^{L} \frac{G(y^+) dy^+}{\frac{1}{\sigma} + \epsilon(y^+)} \equiv I$$

It is anticipated that the results of the analysis will be typically asymptotic in character in the sense that only a few terms will be of use in the calculation. This is a reasonable state of affairs, since more than a few terms of the expansion are very difficult to obtain.

The main part of the analysis involves determining the various σ contributions to the integral I. This is accomplished by using asymptotic procedures (*1*), and these in turn require extensive use of the order symbol O. The notation $O(\sigma^a)$ refers to a quantity that is proportional to σ^a as $\sigma \to \infty$. By establishing the order of the σ dependence of various contributions to I, the appropriate successive major contributions can be extracted. Even when only three terms of the asymptotic expansion are extracted, the calculations become very lengthy and contain many contributions to the final error term. Fortunately, the final products of these lengthy calculations take relatively simple forms.

In order to extract the appropriate contributions to I, the integral

$$J = \int_0^L \frac{x^n \, dx}{\frac{1}{\sigma} + x^p + A x^{p+1} + B x^{p+2}} \quad (24)$$

is of fundamental importance, where L is an arbitrary positive finite upper limit. A knowledge of the asymptotic

Table 1. $G(y^+)$ Variation for Various Situations
For $y^+ \to 0$, $G(y^+) = 1 + b_1 y^+ + b_2 y^{+2} + O(y^{+3})$

Case	b_1	b_2
Parallel plates, constant but unequal temperature	0	0
Parallel plates, constant heat flux	0	$-\dfrac{1}{Re}$
Circular tube, constant heat flux	$\dfrac{2}{Re\sqrt{f/2}}$	$\left(\dfrac{4}{Re^2(f/2)} - \dfrac{4}{Re}\right)$
Concentric annuli, outer wall insulated	$-\dfrac{2(R_2 - R_1)}{R_1 Re\sqrt{f_1/2}}$	$\left(\dfrac{4}{Re^2(f_1/2)}\dfrac{(R_2-R_1)^2}{R_1^2} - \dfrac{4}{Re}\dfrac{R_1}{(R_1+R_2)}\right)$
Concentric annuli, inner wall insulated	$\dfrac{2(R_2 - R_1)}{R_2 Re\sqrt{f_2/2}}$	$\left(\dfrac{4}{Re^2(f_2/2)}\dfrac{(R_2-R_1)^2}{R_2^2} - \dfrac{4}{Re}\dfrac{R_2}{(R_1+R_2)}\right)$

character of J for $\sigma \to \infty$ furnishes the information needed to extract successive contributions in σ from I. The asymptotic behavior of J for $\sigma \to \infty$ depends on the values of p and n. By considering the limit as $\sigma \to \infty$ of J, using the method shown in Appendix B,* it is readily shown that J behaves as indicated in Table 2.

By approximating $\epsilon(y^+)$ in I by a few terms of a power series, the evaluation of I is reduced to the evaluation of several integrals of the form of J. The J integrals are in turn approximated asymptotically for $\sigma \to \infty$. At this point we must address the question of the error incurred by truncating the power series expansion of $\epsilon(y^+)$. The σ dependence of this error is derived in Appendix C.* It turns out that for $\epsilon(y^+)$ beginning with either y^{+3} or y^{+4}, the error incurred by taking three terms in the power series for $\epsilon(y^+)$ is of smaller order in σ than the first three approximations to I, but of the same order as the fourth approximation. Thus, in either of these two cases, to obtain the first three terms of the approximation to I for $\sigma \to \infty$, we must retain three terms in the power series for $\epsilon(y^+)$.

In order to handle the five different $G(y^+)$ variations simultaneously, we write

$$G(y^+) = 1 + b_1 y^+ + b_2 y^{+2} + O(y^{+3}) \qquad (25)$$

where appropriate values of b_1 and b_2 are shown in Table 1 for the various cases of interest. It should be mentioned that even though a particular velocity distribution is assumed in deriving b_1 and b_2, namely the universal velocity profile, the results are not restricted to this velocity distribution. Then I becomes

$$I = \int_{y^+=0}^{L} \frac{1 + b_1 y^+ + b_2 y^{+2} + O(y^{+3})}{\dfrac{1}{\sigma} + \epsilon(y^+)}\, dy^+ + O(1) \qquad (26)$$

where the $O(1)$ contribution comes from replacing the original upper limit by L. This is generally necessary to do since the power series representations of $G(y^+)$ and $\epsilon(y^+)$ might break down for y^+ too large.

The two cases of interest correspond to $\epsilon(y^+)$ beginning as $O(y^{+3})$ and $O(y^{+4})$, respectively, for $y^+ \to 0$. We consider the former case in some detail; the latter case is handled in an entirely analogous manner. We consider $\epsilon(y^+)$ to be expressed as $\epsilon = K_3 y^{+3} + K_4 y^{+4} + K_5 y^{+5}$. Introducing this expression into Equation (25) yields

$$I = \int_{y^+=0}^{L} \frac{1 + b_1 y^+ + b_2 y^{+2} + O(y^{+3})}{\dfrac{1}{\sigma} + K_3 y^{+3} + K_4 y^{+4} + K_5 y^{+5}}\, dy^+ + O(1) \qquad (27)$$

* See footnote on page 527.

The $O(1)$ term in Equation (27) represents the absolute value of the sum of the $O(1)$ term in Equation (26) and the $O(1)$ error arising from the truncation of the power series for ϵ (as explained in Appendix C).

Now we consider individually the four contributions to the integrand of Equation (27). The $O(y^{+3})$ term obviously produces a contribution to the integral of $O(1)$. The quantity $\int 1/(1/\sigma + K_3 y^{+3} + K_4 y^{+4} + K_5 y^{+5})$ has been evaluated by the "successive extraction" process in (5). The result is

$$\int_{y^+=0}^{L} \frac{dy^+}{\dfrac{1}{\sigma} + K_3 y^{+3} + K_4 y^{+4} + K_5 y^{+5}} = \frac{1}{K_3^{1/3}} \left[1.2092\, \sigma^{2/3} - \frac{0.80613\, K_4\, \sigma^{1/3}}{K_3^{4/3}} + \left(\frac{K_4^2}{K_3^{8/3}} - \frac{K_5}{K_3^{5/3}} \right) \frac{\ln \sigma}{3} \right] + O(1) \qquad (28)$$

In a similar way, successive extraction is used to determine the remaining two contributions to I. Some typical details are given in Appendix B. The results of this calculation are

$$\int_{y^+=0}^{L} \frac{y^+ dy^+}{\dfrac{1}{\sigma} + K_3 y^{+3} + K_4 y^{+4} + K_5 y^{+5}} = \frac{1}{K_3^{2/3}} \left[0.6046\, \sigma^{1/3} - \frac{K_4}{3K_3^{4/3}} \ln \sigma \right] + O(1) \qquad (29)$$

and

$$\int_{y^+=0}^{L} \frac{y^{+2} dy^+}{\dfrac{1}{\sigma} + K_3 y^{+3} + K_4 y^{+4} + K_5 y^{+5}} = \frac{\ln \sigma}{3K_3} + O(1) \qquad (30)$$

By putting these results all together, we finally obtain the first three terms of the asymptotic expansion of the Lyon equation for turbulent flow as $\sigma \to \infty$.

$$\frac{\sqrt{f/2}}{St} = C_1 \sigma^{2/3} + C_2 \sigma^{1/3} + C_3 \ln \sigma + O(1)\,. \qquad (31)$$

Here C_1, C_2, and C_3 are

$$C_1 = \frac{1.2092}{K_3^{1/3}} \qquad (32)$$

$$C_2 = \frac{-0.80613\, K_4}{K_3^{5/3}} + \frac{0.6046\, b_1}{K_3^{2/3}} \qquad (33)$$

TABLE 2. ASYMPTOTIC BEHAVIOR OF

$$J = \int_0^L \frac{x^n\,dx}{\frac{1}{\sigma} + x^p + Ax^{p+1} + Bx^{p+2}} \text{ for } \sigma \to \infty$$

For $p - n > 1$, $J = O\left(\sigma^{\left(1 - \frac{1+n}{p}\right)}\right) \to \infty$.
For $p - n = 1$, $J = O(\ln \sigma) \to \infty$.
For $p - n < 1$, $J = O(1) \to$ constant.

$$C_3 = \frac{1}{3}\left\{\left(\frac{K_4^2}{K_3^3} - \frac{K_5}{K_3^2}\right) - \frac{K_4 b_1}{K_3^2} + \frac{b_2}{K_3}\right\} \quad (34)$$

By proceeding in an entirely analogous way, we find that if $\epsilon(y^+)$ varies as $M_4 y^{+4} + M_5 y^{+5} + M_6 y^{+6}$ for y^+ near zero, then the asymptotic expansion of I for $\sigma \to \infty$ becomes

$$\frac{\sqrt{f/2}}{St} = D_1 \sigma^{3/4} + D_2 \sigma^{1/2} + D_3 \sigma^{1/4} + O(\ln \sigma) \quad (35)$$

where

$$D_1 = \frac{1.1107}{M_4^{1/4}} \quad (36)$$

$$D_2 = -\frac{0.39270\,M_5}{M_4^{3/2}} + \frac{0.78540\,b_1}{M_4^{1/2}} \quad (37)$$

$$D_3 = \left(\frac{0.72891\,M_5^2}{M_4^{11/4}} - \frac{0.83304\,M_6}{M_4^{7/4}}\right) - \frac{0.83304\,M_5 b_1}{M_4^{7/4}} + \frac{1.1107\,b_2}{M_4^{3/4}} \quad (38)$$

Results of the Analysis

The foregoing calculations show the effects of Prandtl or Schmidt number, geometry, Reynolds number, and boundary conditions on the downstream Stanton number for turbulent heat or mass transfer in various duct situations when $\sigma \to \infty$.

One of the main objectives of the present study is to accurately assess the effects of these quantities on the Stanton number. The first terms of formulas 31 and 35 have been used a number of times as the $\sigma \to \infty$ asymptote corresponding to various assumptions such as constant radial shear stress, constant radial heat flux and u being nearly u_b over most of the range. The portions of 31 and 35 other than the first term give corrections as a function of σ and Re for various geometries. The effect of Reynolds number, which comes in through b_1 and b_2 is seen to be generally negligible in practice, since the results are valid in general only for $Re \geqq 10^4$. This is true for all geometries considered. The importance of the σ corrections cannot be determined from the previous analysis alone, since the magnitudes of the various constants in the $\epsilon(y^+)$ expression are unspecified and also the magnitudes of the errors $O(1)$ and $O(\ln \sigma)$ in Equations (31) and (35) are unknown. An assessment of the importance of the various σ contributions is made in the next section. The preceding calculations together with Appendix A show that for parallel plates, tubes and annuli the Stanton number is independent of whether the boundary condition is constant temperature or constant flux, if proper scaling is used.

Numerical Comparison

In order to determine the relative importance of the various σ contributions in the asymptotic expansion and also to estimate the error term, we have recourse to a numerical example. Since we must adopt a specific $\epsilon(y^+)$ distribution for the comparison, we choose the following simple relationship due to Wasan, Tien, and Wilke (*13*).

$$\epsilon(y^+) = \frac{4.16 \times 10^{-4} y^{+3} - 15.15 \times 10^{-6} y^{+4}}{1 - 4.16 \times 10^{-4} y^{+3} + 15.15 \times 10^{-6} y^{+4}} \quad (39)$$

Wasan and Wilke (*14*) integrate $1/(1/\sigma + \epsilon(y^+))$ from $y^+ = 0$ to 20 using Equation (39), and we consider the same procedure. From Equation (39), we see that $K_3 = 4.16 \times 10^{-4}$, $K_4 = -15.15 \times 10^{-6}$, and $K_5 = 0$. Also, for this numerical example we have $b_1 = 0$ and $b_2 = 0$ in Equation (31).

Because of the rapid variation of the integrand near $y^+ = 0$ for large σ, particular care is necessary in evaluating the integral numerically. The integral was broken up into appropriate portions corresponding to proper scaling, but even then roundoff error caused some difficulty using single precision. An error monitoring procedure was used together with double precision arithmetic to produce the numerical results of Table 3. Fortunately, owing to algebraic simplifications the integral can be evaluated exactly for $\sigma = 1$. For this case it is equal to 13.056, which compares well with the approximate numerical value 13.05601. By virtue of this check and the numerical agreement for $\sigma \to \infty$, the numerical results are thought to be much more accurate than the number of figures shown in Table 3.

The comparison of the numerical integration and Equation (31) in Table 3 shows good agreement for large σ values. We consider σ values up to 10^5, since this represents about the largest values thus far obtained experimentally. According to Equation (31), the error of the approximate formula should approach a constant as $\sigma \to \infty$. Inspection of the difference between the predicted and numerical values shows that the difference goes steadily from 22.7 at $\sigma = 10^4$ to 23.1 at $\sigma = 10^5$, which suggests that the limit (to three significant figures) is about 23.1. If this experimental constant value is incorporated into the approximate formula, the agreement between approximation and numerical values is extremely good. This example indicates that at least the correction term $O(\sigma^{1/3})$ is important in the approximation when ordinary accuracies are sought.

The example also shows clearly that approximation [Equation (31)] could be used to evaluate the integral used by Wasan and Wilke in a Prandtl-Taylor type development. If the upper limit of the integral had corresponded

TABLE 3. COMPARISON OF NUMERICAL INTEGRATION OF

$$\int_0^{20} \frac{dy^+}{\frac{1}{\sigma} + \epsilon(y^+)}$$

With Approximation Formula 31 for $\epsilon(y^+)$ from (*13*)

σ	$I_{\text{approx.}}$	$I_{\text{numerical}}$	$I_{\text{approx.}}$*
1‡	21.5	13.05601	
10	89.0	73.9	65.9
50	243.4	225.0	220.3
100	378.3	358.9	355.2
500	1068.8	1047.7	1045.7
1000	1679.8	1658.2	1656.7
5000	4835.5	4813.1	4812.4
10000	7641.8	7619.1	7618.7
50000	22190.0	22167.0	22167.0
100000	35155.0	35132.0	35132.0

‡ *the exact value of I at σ = 1 is 13.056*
* with "experimental" constant added in

to integrating over the entire transport region, the constant value would be larger and would actually vary somewhat with Reynolds number.

Another way to effectively determine the unknown coefficient of $\epsilon(y^+)$ near $y^+ = 0$ is to assume that the values in the preceding numerical example are approximately correct, which suggests that the approximation formulae [Equations (31) and (35)] are valid for $\sigma \to \infty$, and then use large σ experimental results to find the constants. This approach is used in the next section.

COMPARISON WITH EXPERIMENTAL DATA

The recent high Schmidt number mass transfer data of Harriott and Hamilton (*6*) covers a wide range in Schmidt number (400 to 100,000) and afford an opportunity to test the capability of the derived equations to fit experimental data. A comparison with experimental data will permit a determination of the constants appearing in the eddy diffusivity expressions and should allow a distinction to be made between ϵ^+ varying as y^{+3} or y^{+4} for the limit as $y^+ \to 0$.

Equations (31) and (35) may be put in the form of Equation (40). Equation (40) neglects the Reynolds number dependence of the constants which is seen to be extremely small.

$$St = \frac{\sqrt{f/2}}{B_1 Sc^{1-1/n} + B_2 Sc^{1-2/n} + B_3 F(n)} \qquad (40)$$

where

$$F(3) = \ln(Sc)$$

$$F(4) = Sc^{1/4}$$

The Harriott and Hamilton (*6*) data (58 points) were fitted to Equation (40) using a nonlinear least squares procedure. The results of these calculations are shown in Table 4. The mean and standard deviations shown in Table 4 are defined as

$$\text{mean deviation} = \frac{1}{N} \sum_{i=1}^{N} \left| \frac{St_{\text{pred.}} - St_{\text{exp.}}}{St_{\text{exp}}} \right| \qquad (41)$$

standard deviation

$$= \left[\frac{1}{N-3} \sum_{i=1}^{N} \left(\frac{St_{\text{pred.}} - St_{\text{exp.}}}{St_{\text{exp}}} \right)^2 \right]^{1/2} \qquad (42)$$

From these results it is seen that $n = 3$ does a better job of fitting the data than does $n = 4$; however, the differences are not large. It would thus appear that the precision of the data does not allow a distinction to be made as to whether ϵ begins with y^{+3} or y^{+4}; however, the formulas derived in this work should allow a resolution of this problem when high precision data become available.

The data are shown compared to Equation (40) for $n = 3$ in Figure 2.

From the results of the least squares analysis of the mass transfer data, the expressions for the eddy diffusivity in the wall region are determined as

TABLE 4. COMPARISON WITH EXPERIMENTAL DATA

n	B_1	B_2	B_3	Mean deviation (%)	Standard deviation (%)
3	12.62	1.881	0.2341	5.42	6.90
4	4.560	14.32	1.081	6.41	8.48

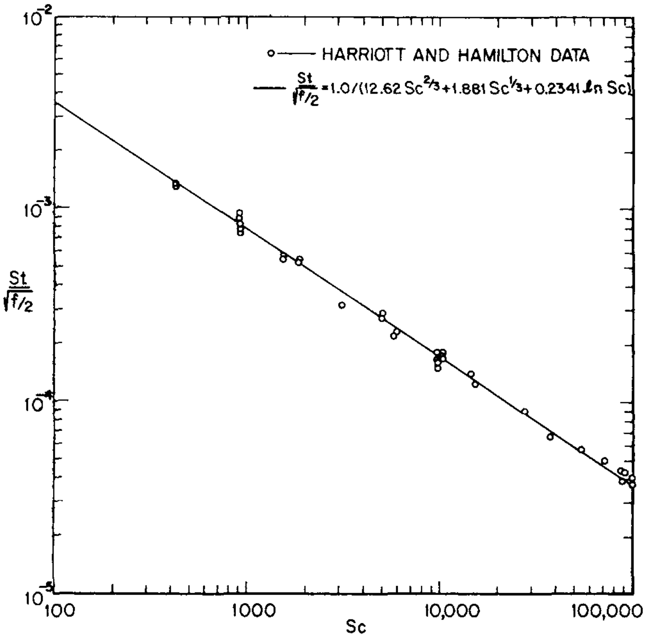

Fig. 2. Comparison with experimental data.

$$\epsilon = 8.800 \times 10^{-4} y^{+3} - 1.885 \times 10^{-5} y^{+4} - 1.398 \times 10^{-7} y^{+5} \qquad (43)$$

and

$$\epsilon = 3.522 \times 10^{-3} y^{+4} - 7.621 \times 10^{-3} y^{+5} + 1.436 \times 10^{-2} y^{+6}. \qquad (44)$$

CONCLUSIONS

High Prandtl or Schmidt number asymptotic formulae have been derived for the Stanton number in turbulent duct flows. It is shown that in the limit of large Prandtl numbers, the results are equivalent for the parallel plate, circular tube, and concentric annuli geometries. In addition, it is seen that the boundary conditions of constant wall heat flux and constant wall temperature also give equivalent results. The theoretical expressions derived show good agreement with typical numerical calculations down to relatively low σ values. A comparison of the formulae obtained with recent large Schmidt number mass transfer data shows good agreement. The correction terms to the $\sigma \to \infty$ asymptote are more important for either $\epsilon \propto y^{+4}$ or for smaller values of σ. The comparison with experimental data does not give conclusive evidence for ϵ varying either as y^{+3} or y^{+4} in the limit of $y^+ \to 0$.

ACKNOWLEDGMENT

Acknowledgment is made to the Research Committee and the Computer Center of the University of California, Santa Barbara, for support of this research in the form of computer time.

NOTATION

b_1, b_2 = coefficients of power series expansion for $G(y^+)$, $G(y^+) = 1 + b_1 y^+ + b_2 y^{+2} + O(y^{+3})$
B_1, B_2, B_3 = constants in Equation (40)
f = friction factor, $f = 2\tau_w/\rho u_b^2$
f_1, f_2 = friction factor corresponding to wall 1 and wall 2 for annulus
$G(y^+)$ = numerator of integrand for I
h = heat transfer coefficient defined by Equation (5)
I = integral describing turbulent Stanton number,

$$I = \int_0^L \frac{G(y^+)}{1/\sigma + \epsilon(y^+)} dy^+$$

k = thermal conductivity
K_3, K_4, K_5 = coefficients in Taylor series expansion for ϵ beginning with y^{+3}
L = upper integration limit for I
M_4, M_5, M_6 = coefficients in Taylor series expansion for ϵ beginning with y^{+4}
n = exponent on y^+ in first term of ϵ expansion
$O(\ )$ = order symbol, $A = O(\sigma^a) \rightarrow A \propto \sigma^a$, for $\sigma \rightarrow \infty$
P_k = coefficients in Taylor series expansion for ϵ
q_w = wall heat flux
r^+ = dimensionless radial coordinate, $r^+ = ru^*/\nu$
R^+ = dimensionless tube radius, $R^+ = Ru^*/\nu$
R_1^+, R_2^+ = dimensionless radii for annulus, $R_1^+ = R_1u^*/\nu$, $R_2^+ = R_2u^*/\nu$
Re = Reynolds number, $Re = 2Ru_b/\nu$, for tube, $Re = 2Yu_b/\nu$, for parallel plates, $Re = \frac{2(R_2 - R_1)u_b}{\nu}$ for annulus
St = Stanton number, $St = h/\rho C_p u_b$
St_T = Stanton number for constant temperature boundary conditions
u^+ = dimensionless velocity, $u^+ = u/u^*$
u^* = friction velocity, $u^* = u_b\sqrt{f/2}$
u_b = bulk velocity
x^+ = dimensionless axial distance, $x^+ = xu^*/\nu$
y^+ = dimensionless distance from wall, $y^+ = yu^*/\nu$
Y^+ = dimensionless channel half-width, $Y^+ = Yu^*/\nu$
α = constant defined by Equation (10)
ϵ = dimensionless eddy diffusivity, $\epsilon = E_H/\nu$
ν = kinematic viscosity
σ = Prandtl or Schmidt number
θ = temperature
θ_0 = upstream temperature at $x = 0$
θ_1, θ_2 = wall temperatures
θ^+ = dimensionless temperature
θ_b = bulk temperature
θ_b^+ = dimensionless bulk temperature
θ_c = centerline temperature

LITERATURE CITED

1. De Bruijn, N. G., "Asymptotic Methods in Analysis," North-Holland, Amsterdam (1961).
2. Deissler, R. G., NACA Tech. Note, 3145 (1954).
3. Elrod, H. G., *J. Aero. Sci.*, **24**, 468 (1957); erratum, **27**, 145 (1960).
4. Friend, W. L., and A. B. Metzner, *AIChE J.*, **4**, 393 (1958).
5. Hanna, O. T., paper presented at Am. Inst. Chem. Engrs. 63rd Annual Meeting, Chicago (1970).
6. Harriott, P., and R. M. Hamilton, *Chem. Eng. Sci.*, **20**, 1073 (1965).
7. Hubbard, D. W., and E. N. Lightfoot, *Ind. Eng. Chem. Fundamentals*, **5**, 370 (1966).
8. Knudsen, J. G., and D. L. Katz, "Fluid Dynamics and Heat Transfer," McGraw-Hill, New York (1958).
9. Lin, C. S., R. W. Moulton, and G. L. Putnam, *Ind. Eng. Chem.*, **45**, 636 (1953).
10. Lyon, R. N., *Chem. Eng. Progr.*, **47**, 75 (1951).
11. Seban, R. A., and T. T. Shimazaki, *Trans. A.S.M.E.*, **73**, 803 (1951).
12. Son, J. S., and T. J. Hanratty, *AIChE J.*, **13**, 689 (1967).
13. Wasan, D. T., C. L. Tien, and C. R. Wilke, *AIChE J.*, **9**, 567 (1963).
14. Wasan, D. T., and C. R. Wilke, *Intern. J. Heat Mass Transfer*, **7**, 87 (1964).

Manuscript received May 27, 1971; revision received October 21, 1971; paper accepted October 26, 1971.

An Efficient Algorithm for Optimum Decomposition of Recycle Systems

RAVINDRA S. UPADHYE and EDWARD A. GRENS II

Department of Chemical Engineering
University of California, Berkeley, California 94720

A method is developed for decomposition of a recycle process so as to minimize the summation of weighting factors for variables torn. This procedure is based on application of dynamic programming to a state space representing combinations of cycles opened. The resulting algorithm is well suited to machine implementation and is more efficient for large problems than alternative procedures that also guarantee decomposition.

Most chemical processes are characterized by recycle of material and/or energy. In addition, the units in a process are in general nonlinear. These characteristics usually combine to preclude direct solution to mathematical models for entire processes in the course of analysis or simulation of the process.

Correspondence concerning this paper should be addressed to E. A. Grens II.

The presence of recycle streams requires the equation system representing several or all process units to be treated simultaneously. It is not possible to proceed directly with the calculation of units in any order, since the output of some units will be inputs to previous units in the sequence. Moreover, since the large number of equations that must be solved simultaneously are not linear, it is necessary to resort to iterative methods for the calculation of the variables involved in the process streams. These